

# PHYSICAL REVIEW B

## CONDENSED MATTER

THIRD SERIES, VOLUME 41, NUMBER 16

1 JUNE 1990

### Effect of nonmagnetic impurities on the residual electron-spin-resonance linewidth of Er:Ag dilute alloys

E. D. Dahlberg,\* J. Souletie,<sup>†</sup> S. A. Dodds,<sup>‡</sup> E. P. Chock, and R. L. Orbach

*Department of Physics, University of California, Los Angeles, California 90024*

(Received 18 December 1989)

We have undertaken a systematic investigation of the effect of nonmagnetic impurities on the residual ( $T \rightarrow 0$  K) electron-spin-resonance linewidth of erbium in dilute [200 parts per million atomic (ppm)] Er:Ag alloys. The nonmagnetic impurities used were In, Sn, Sb, Y, and Lu in the concentration range of 500–4600 ppm. The linewidth broadening caused by these impurities was found to be  $0.2 \pm 0.11$ ,  $0.49 \pm 0.1$ ,  $0.51 \pm 0.11$ ,  $1.4 \pm 0.18$ , and  $1.37 \pm 0.32$  G/1000 ppm atomic frequency (GHz) for In, Sn, Sb, Y, and Lu, respectively. The most reasonable source of the Er line broadening is the mixing of the crystal-field levels of the Er by the Kohn-Vosko oscillations in the charge density. The broadening of the Er resonance line due to In, Sn, and Sb doping is consistent with the expected form of the oscillations. Also, Y and Lu are equivalent in the broadening of the Er line, as expected. However, the scaling of the Y and Lu broadening compared to that due to the In, Sn, and Sb is not consistent. The reasons for this are not understood.

#### I. INTRODUCTION

In a previous publication<sup>1</sup> (hereafter referred to as I) the residual ( $T \rightarrow 0$  K) electron-spin-resonance (ESR) linewidth of dilute Er:Ag alloys was investigated by varying the erbium concentration and making ESR measurements at two well separated frequencies (9 and 1.6 GHz). The residual linewidth was found to be linear in the Er concentration at both frequencies but the slopes of the residual linewidth versus Er concentration were not equal nor did they scale with frequency. It was assumed that there was both frequency-dependent and frequency-independent broadening associated with the Er concentration. In I it was shown that the homogeneous broadening could be explained by magnetic dipole-dipole interactions between the Er spins. The frequency-dependent broadening was assumed to be due to Kohn-Vosko<sup>2</sup> oscillations in the charge density of the screening electrons around the charged impurity. In order to further investigate this broadening mechanism we have undertaken a systematic investigation of the effect of Kohn-Vosko charge oscillations or electric-field gradients (EFG's) on the ESR of 200 parts per million atomic (ppm) Er:Ag alloys with either In, Sn, Sb, Y or Lu as a second impurity in the concentration range of 500–4600 ppm.

In Sec. II we present the experimental procedures utilized and the experimental data. The data are compared with the expected EFG's in Sec. III, and our conclusions are in Sec. IV.

#### II. EXPERIMENTAL TECHNIQUES AND RESULTS

Master alloys of 1% atomic Er:Ag and X:Ag (where X is In, Sn, Sb, Y, or Lu) were prepared in an arc furnace under an argon atmosphere. Portions of these alloys were mixed with each other and with silver in the arc furnace to make samples containing 200 ppm Er and from 500 to 4000 ppm of X. The samples were homogenized by rf induction heating for 1 h, at slightly above the liquidus temperature and finally annealed for 8 h at 800°C. The concentrations of the In, Sn, and Lu codopants in each of the samples used for the ESR measurements were checked by neutron activation and the codopant concentrations will be taken as those thus determined. The concentration of the Y in the ESR samples will be taken as the nominal concentration. The Sb codoped samples present more of a problem and will be discussed later.

Samples were filed with a tungsten carbide file to make powders for the ESR measurements. The ESR of the Er was measured at 9.2 GHz on all the samples as a function of temperature from 4.2 to 1.4 K (seven temperatures over this range). The 2000 ppm Lu sample was also measured in a 1.7 GHz ESR spectrometer<sup>3</sup> in the same temperature range to verify that the induced broadening was due to a distribution of Er g values.

The residual linewidth was determined by plotting the measured linewidth versus temperature (determined in the manner of Peter *et al.*<sup>4</sup> using a Lorentzian line shape) for each concentration of each second impurity and

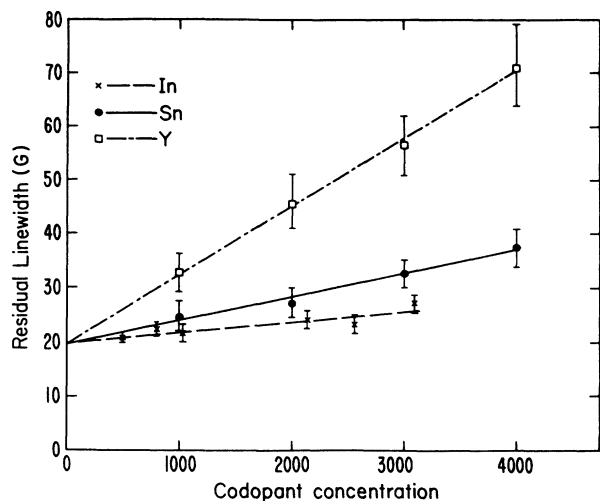


FIG. 1. Change in the residual ( $T=0$  K) linewidth as a function of the concentration (in ppm) of a charge impurity (In, Sn, Y).

linearly extrapolating to  $T=0$  K. In general, the slope of the linewidth versus temperature plots agreed within the error bars with those published elsewhere.<sup>5</sup> The exception was in the higher concentrations of Y and Lu. It was also found for those samples that the central portions of the ESR spectra were no longer completely Lorentzian. This could explain an erroneous temperature dependence of the linewidth, and a small shift in the measured  $g$  value. These problems were quantitatively insignificant and will not be discussed further. The  $T=0$  K intercept of the linewidth versus temperature plot is defined as the residual linewidth. The residual linewidth for each codopant was then plotted as a function of concentration and is presented in Figures 1 and 2 together with a least-squares fit to a straight line.

From I, the ESR residual linewidth of a filled 200 ppm atomic Er:Ag alloy should be 19–20 G at 9.2 GHz. The data presented show that the extrapolated zero concentration residual linewidth for each second impurity lies close to this value with the exception of Sb, which is 2.5–3.5 G larger than it should be. However, if we consider only Sb concentrations  $\leq 2000$  ppm atomic, then the intercept is in the proper range. This behavior prob-

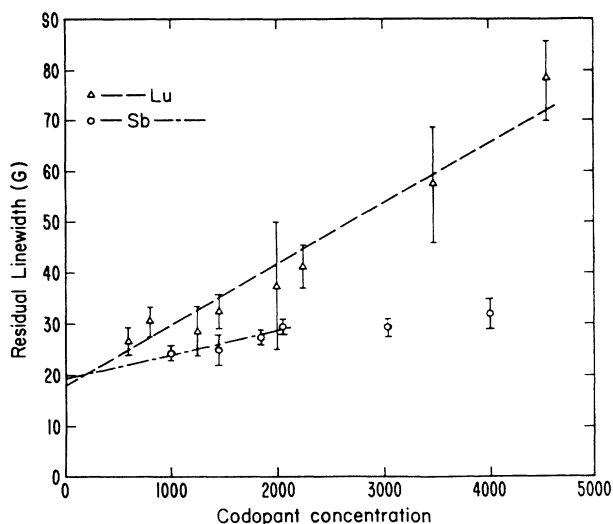


FIG. 2. Change in the residual ( $T=0$  K) linewidth as a function of the concentration (in ppm) of a charge impurity (Sb, Lu). Only the Sb concentrations less than 2000 ppm were considered (see the text).

ably indicates a loss of Sb and therefore our analysis will be limited to Sb concentrations of 2000 ppm or less.

The data in Figs. 1 and 2 can be represented by a function of the form  $a + bcf$ , where  $a$  depends on Er concentration and lattice strain,<sup>1</sup>  $b$  is proportional to the impurity-induced EFG,  $c$  is the codopant concentration, and  $f$  is the measuring frequency. As already noted, the value of  $a$  is a constant, appropriate to the 200 ppm Er concentration. The values of  $b$  for each codopant are listed in the last column of Table I.

### III. THEORY AND COMPARISON OF EXPERIMENTAL RESULTS

The ESR spectrum of Er:Ag arises from an isolated  $\Gamma_7$  ground-state doublet. The first excited state is a  $\Gamma_8^{(1)}$  and the two are separated in energy by approximately 35 K.<sup>6</sup> The  $\Gamma_7$  ground-state spectrum of Er has an isotropic  $g$  value of 6.8,<sup>7</sup> but a small admixture of the  $\Gamma_8^{(1)}$  state can alter the observed  $g$  value slightly. If the admixture varies randomly over a large number of Er sites, the re-

TABLE I. The ionic radii are taken from Ref. 12, p. 129 and Ref. 17.  $\Delta Z_{\text{eff}}$  is calculated from Eq. (4).  $A_{\text{scaled}}$  is the  $A$  value scaled to the solid line curve in Fig. 3. One should note that the measured values of ESR line broadening ( $\Delta H$  residual) correlate with  $A$ , not the ionic radii.

Impurity	Ionic radii ( $\text{\AA}$ )	$\Delta Z$	$\Delta Z_{\text{eff}}$	$A$	$A_{\text{scaled}}$	$b$ (see the text) [G/1000 ppm $f$ (GHz)]
In <sup>3+</sup>	0.92	2	1.84	0.033	0.22	0.2 $\pm$ 0.11
Sn <sup>4+</sup>	0.74	3	2.75	0.064	0.42	0.49 $\pm$ 0.1
Sb <sup>5+</sup>	0.62	4	3.65	0.09	0.59	0.51 $\pm$ 0.11
Y <sup>3+</sup>		2		0.106	0.74	1.4 $\pm$ 0.18
Lu <sup>3+</sup>	0.93 <sup>a</sup>	2		0.106	0.74	1.37 $\pm$ 0.32
Er <sup>3+</sup>	0.96	2		0.106	0.74	2.1 $\pm$ 0.8
Ag <sup>+</sup>	1.13	0				

<sup>a</sup>By extrapolation.

sult will be a broadened Er ESR spectrum. Because the resonance line is constructed from a distribution of  $g$ -shifted lines, we would expect the observed linewidth to scale with the frequency of measurement. The  $\Gamma_7\text{-}\Gamma_8^{(1)}$  mixing can be generated by virtue of the presence of EFG's caused by charged impurities in the host. These would be the Er ions themselves in I. In the present work there are two contributions: One due to the second im-

$$A = \frac{1}{2\pi^2} \left[ \left( \sum_l (2l+1) [-\sin\eta_l \cos(\eta_l - l\pi)] \right)^2 + \sum_l (2l+1) [-\sin\eta_l \sin(\eta_l - l\pi)]^2 \right]^{1/2} \quad (1)$$

for a free-electron conduction band. The phase shifts  $\eta_l$  are constrained by the Friedel sum rule

$$\Delta Z = (2/\pi) \sum_{l=0}^{\infty} (2l+1)\eta_l, \quad (2)$$

where  $\Delta Z$  is the valence difference between the host and impurity. Additional information is obtained from the residual electrical resistivity<sup>8</sup> caused by the impurities  $\Delta\rho$ , given by

$$\Delta\rho = (2hc/k_F e^2) \sum_{l=1}^{\infty} l \sin^2(\eta_{l-1} - \eta_l), \quad (3)$$

where  $h$  is Planck's constant,  $c$  is the velocity of light,  $k_F$  is the Fermi wave vector and  $e$  is the charge of an electron.

In principle, the phase shifts can be determined by solving a set of simultaneous equations such as those above. For the work here, however, the calculations of Hurd and Gordon<sup>9</sup> have been utilized. They used a semi-empirical method to model the potential of several period five elements (including In, Sn, and Sb) dissolved in the noble metals. Using an effective charge difference ( $\Delta Z_{\text{eff}}$ ) or valence for the solute atoms as developed by Blatt,<sup>10</sup> their analysis revealed that only the  $l=0, 1$ , and 2 partial waves were important for the various alloys. More important for the present work, a plot of their calculated phase shifts for  $l=0$  and 1 versus  $\Delta Z_{\text{eff}}$  is linear. The phase shift associated with the  $l=2$  partial wave is linear for  $\Delta Z_{\text{eff}}$  less than two and for values of  $\Delta Z_{\text{eff}}$  greater than two this phase shift assumes a constant value. This systematic variation of the phase shifts as a function of  $\Delta Z_{\text{eff}}$  allows the calculation of any physical property that is a function of the scattering from the solvent ions as a continuous function of  $\Delta Z_{\text{eff}}$ .

As previously mentioned, the use of a  $\Delta Z_{\text{eff}}$  was first considered by Blatt. He argued that the charge used in the Friedel sum rule is not the atomic valence difference between the host and impurity ions, but rather the change in the electronic charge in a unit cell that considers both valence differences and the difference of radii of the host and the impurity ions. He concludes  $\Delta Z$  in (2) should be replaced with  $\Delta Z_{\text{eff}}$  given by

$$\Delta Z_{\text{eff}} = \Delta Z - (\delta a/a)(1+\sigma)/(1-\sigma), \quad (4)$$

where  $\sigma$  is Poisson's ratio for the host lattice and  $(\delta a/a)$

purity and the other to the (constant) 200 ppm concentration of Er.

The magnitude of the oscillations in the conduction electron density which generate the EFG's can be calculated from a knowledge of the charged impurity scattering phase shifts at the Fermi surface,  $\eta_l$ . Kohn and Vosko<sup>2</sup> found that the EFG's are proportional to

is the fractional change in the lattice constant per atomic percent impurity. This argument is useful in explaining the resistivity of impurity ions in systems where the impurity and host ions have the same valence.

For the silver alloys reported here, the  $\Delta Z_{\text{eff}}$ 's can be determined from the value of Poisson's ratio for silver (0.43),<sup>11</sup> the lattice constant of silver (4.09 Å) (Ref. 12) and the fractional change in the lattice constant per atomic percent In, Sn, and Sb which are taken to be 0.34, 0.42, and 0.62 respectively.<sup>13</sup> From these numbers the  $\Delta Z_{\text{eff}}$ 's are 1.84, 2.75, and 3.65 for In, Sn, and Sb, respectively. Using the  $\Delta Z_{\text{eff}}$ 's and the graphs of the various  $\eta_l$  versus  $\Delta Z_{\text{eff}}$  calculated in Ref. 9, we have determined the appropriate phase shifts for In, Sn, and Sb. Using these phase shifts and Eq. (1) the magnitude of the  $A$ 's necessary for the determination of the EFG's were found to be 0.033, 0.064, and 0.09, respectively.

As mentioned previously, the phase shifts vary in a continuous fashion with the charge difference in a unit cell and thus the magnitude of the charge density oscillation also varies continuously. It is this approach we have used in Fig. 3. There we exhibit the observed change in the residual linewidth per 1000 ppm impurity-frequency

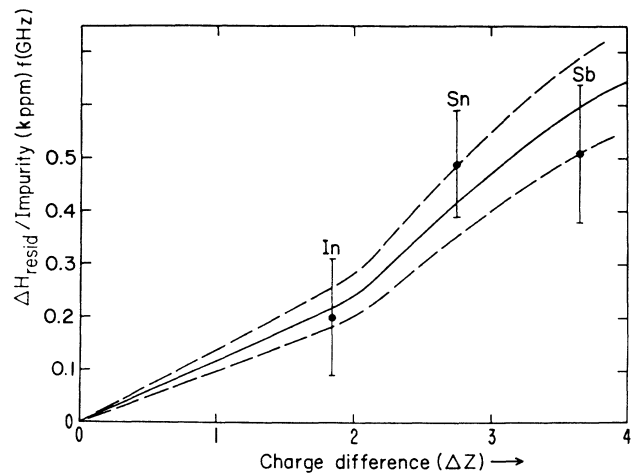


FIG. 3. Slopes of the straight line fits in the In, Sn, and Sb data in Figs. 3 and 4 as a function of effective charge difference. The lower dashed curve is the magnitude of the charge-density oscillations scaled to the Sb data. The upper dashed curve is scaled to the Sn data and the solid curve is fit to all three (In, Sn, and Sb).

(GHz) plotted against the effective charge difference. Since a detailed theory for the effect of EFG on the ESR of a local moment in a metal is lacking, we have scaled the calculated magnitudes of the EFG to the experimental data. The lower curve has been scaled to the Sb data, the upper curve to the Sn data with the solid curve being a fit to all three impurities. As mentioned before, this curve is not an absolute fit, but rather a fit to the functional form of the magnitude of the charge-density oscillations.

For the Y, Lu, and Er solutes, we have used  $\Delta Z = 2$ . The resistivity is taken to be  $6.0 \mu\Omega \text{ cm/at\%}$ , as measured for Er. The  $l=0,2$  phase shifts, appropriate for the  $s^2d^1$  configuration, can then be calculated from Eqs. (2) and (3). The resulting values of  $A$  are listed in Table I, together with the scaled values obtained by using the same factor as for In, Sn, and Sb. Table I exhibits a comparison of the observed broadening of the impurities and the magnitude of the charge-density oscillations scaled to the solid curve in Fig. 3.

There are two aspects of this comparison which deserve mention. The first is that there appears to be a discrepancy between the broadening caused by Er and that due to Y or Lu. In I, the experimentally determined contributions to the residual linewidth were found to be  $8.0 \pm 5.0 \text{ G/1000 ppm Er}$  for the dipole-dipole interaction linewidth and  $2.1 \pm 0.8 \text{ G/1000 ppm Er-f(GHz)}$  for the charge-density broadening. If we assume the dipole-dipole interaction linewidth to be the theoretical value of  $12.5 \text{ G/1000 ppm Er}$  as calculated in I, then the charge-density broadening would be reduced to  $1.6 \text{ G/1000 ppm Er-f(GHz)}$ , which is consistent with the value found experimentally in the present work for Y and Lu of about  $1.4 \text{ G/1000 ppm-f(GHz)}$ . This reanalysis of the Er dependent broadening is still within the error bars of the values quoted in I and thus may present a more realistic view of the Er self-generated residual linewidth.

The second aspect is the large difference between the Y-Lu-Er data and the scaled magnitude of the associated charge-density oscillations. With a knowledge of the phase shifts and the linewidth broadening associated with a given impurity, one should be able to predict the linewidth broadening associated with a second impurity with only a knowledge of the scattering phase shifts. This is the essence of the fit to the functional form of the charge-density oscillations shown in Fig. 3. For these impurities (In, Sn, and Sb) the charge difference is systematically changed by increasing the number of  $p$  electrons of the impurity with In, Sn, and Sb having one, two, and three  $p$  valence electrons, respectively. Thus if the number or orbital character of the valence electrons is changed, one should be able to predict the linewidth broadening in the following manner. First, determine the scattering phase shifts from the Friedel sum rule and the residual resistivity associated with the impurity. From the phase shifts one can calculate the magnitude of the charge-density oscillations  $A$  given by the theory of Kohn and Vosko. By scaling this value of  $A$  with the value of  $A$  when the linewidth broadening is known one should be able to predict the residual linewidth.

The above is the approach taken in determining  $A_{\text{scaled}}$

in Table I. The  $A$ 's calculated from the phase shifts for In, Sn, and Sb were multiplied by a constant to give values appropriate to the solid curve in Fig. 3. This scaling factor was then multiplied by the  $A$ 's calculated for Y, Lu, and Er and should have agreed with the experimentally determined broadening associated with these impurities. However, as can be seen by comparing the last two columns in Table I, the  $A_{\text{scaled}}$  values for Y, Lu, and Er are smaller than the observed values of the broadening by roughly a factor of 2. Thus it would appear that one can scale the broadening with an increase in the number of electrons of a given orbital character across a series (i.e., In, Sn, and Sb) but it appears this cannot be done if the orbital character of the screened valence electrons is altered (i.e., change the  $p$ -like electrons of In, Sn, and Sb to the  $d$ -like electrons of Y, Lu, and Er). The reason for this discrepancy is not understood, other than the obvious connection with the difference in the charge configuration ( $s^2p^x$  vs  $s^2d^1$ ) between the two sets of impurities. Even when satisfying only the Friedel sum rule (neglecting the observed resistivities) for the Y, Lu, and Er, a set of phase shifts could not be determined which increased  $A_{\text{scaled}}$  to the magnitude of the observed broadening.

A second effect of the impurities is to generate strains in the silver lattice. These strains will also broaden the ESR line.<sup>14,15</sup> This broadening should scale with the magnitude of the strain that is proportional to the ionic radius of the given impurity or dopant. That this strain induced broadening is not the main contribution to the frequency-dopant broadening of the Er line may be determined by inspecting Table I. The columns of interest in this table, for the question of the strain broadening, are the ionic radii column and the last column which is the experimentally determined solute induced broadening. For example, of all the dopants, the Lu and Er ions are the closest in size to Ag but generate the maximum broadening. This indicates strain is not responsible for the observations. Also, a comparison of the relative broadening of the In, Sn, and Sb dopants also leads one to the conclusion that the observed broadening is not strain induced.

Summarizing, we have shown that the functional form of the frequency dependent Er ESR broadening for In, Sn, and Sb impurities is consistent with the EFG model and that, as expected, Er, Y, and Lu produced equivalent broadening of the Er line. The difficulty comes in comparing the In, Sn, and Sb induced broadening to that produced by the Er, Y, and Lu. What is unclear is whether the actual charge configuration, as well as  $\Delta Z$ , is important in determining the broadening or if a mechanism different from the EFG's are responsible.<sup>16</sup> In either case, it is apparent that our simple phase-shift treatment does not adequately describe the data.

#### ACKNOWLEDGMENTS

One of the authors (E.D.D.) would like to thank C. Foiles and S. Barnes for many interesting conversations. This research was funded in part by National Science Foundation (NSF) Grant No. DMR 86-18968.

\*Present address: School of Physics and Astronomy, University of Minnesota, Minneapolis, Minnesota 55455.

†Permanent address: CNRS/CRTBT Centre de Tri, 38042 Grenoble CEDEX, France.

‡Present address: Department of Physics, Rice University, Houston, Texas 77251.

<sup>1</sup>E. D. Dahlberg, *Phys. Rev. B* **16**, 170 (1977).

<sup>2</sup>W. Kohn and S. H. Vosko, *Phys. Rev.* **119**, 912 (1960).

<sup>3</sup>E. D. Dahlberg and S. A. Dodds, *Rev. Sci. Instrum.* **52**, 472 (1981).

<sup>4</sup>M. Peter, D. Shatiel, J. H. Wernick, H. J. Williams, J. B. Mock, and R. C. Sherwood, *Phys. Rev.* **126**, 1395 (1962).

<sup>5</sup>D. Davidov, C. Rettori, A. Dixon, K. Baberschke, E. P. Chock, and R. Orbach, *Phys. Rev. B* **8**, 3563 (1973).

<sup>6</sup>G. Williams and L. L. Hirst, *Phys. Rev.* **185**, 407 (1969).

<sup>7</sup>L. L. Hirst, G. Williams, D. Griffiths, and R. R. Coles, *J. Appl. Phys.* **39**, 840 (1968).

<sup>8</sup>J. M. Ziman, *Principles of the Theory of Solids*, 2nd ed. (Univer-

sity Press, Cambridge, 1972).

<sup>9</sup>C. M. Hurd and E. M. Gordon, *J. Phys. Chem. Solids* **29**, 2205 (1968).

<sup>10</sup>F. J. Blatt, *Phys. Rev.* **108**, 285 (1957).

<sup>11</sup>D. Arbilly, G. Deutscher, E. Grunbaum, R. Orbach, and J. T. Suss, *Phys. Rev. B* **12**, 5068 (1975).

<sup>12</sup>C. Kittel, *Introduction to Solid State Physics*, 4th ed. (Wiley, New York, 1971), p. 38.

<sup>13</sup>W. B. Pearson, *Lattice Spacings and Structures of Metals and Alloys* (Pergamon, New York, 1958), p. 263.

<sup>14</sup>S. B. Oseroff and R. Calvo, *Phys. Rev.* **18**, 3041 (1978).

<sup>15</sup>Y. von Spalden and K. Baberschke, *J. Magn. Magn. Mater.* **23**, 183 (1981).

<sup>16</sup>Some rather novel broadening mechanisms and mechanisms that do not cause broadening are reviewed by S. E. Barnes, *Adv. Phys.* **30**, 801 (1981). See Sec. 3.6.

<sup>17</sup>R. D. Shannon and C. T. Prewitt, *Acta Crystallogr. B* **25**, 925 (1969).